# Intermediate-valent Cerium in $Ce_2Ru_4Mg_{17}$ and a Group-Subgroup Scheme for $La_9Ru_4In_5$ and $Ce_9Ru_4Ga_5$

Stefan Linsinger, Rolf-Dieter Hoffmann, Matthias Eul, and Rainer Pöttgen

Institut für Anorganische und Analytische Chemie, Universität Münster, Corrensstraße 30, 48149 Münster, Germany

Reprint requests to R. Pöttgen. E-mail: pottgen@uni-muenster.de

*Z. Naturforsch.* **2012**, *67b,* 219 – 225; received February 24, 2012

$Ce_2Ru_4Mg_{17}$ was synthesized by high-frequency melting of the elements in a sealed tantalum ampoule. This magnesium-rich compound crystallizes with a new tetragonal structure type: $I\bar{4}2m$, $a$ = 986.75(8), $c$ = 1008.7(1) pm, $wR2$ = 0.0513, 909 $F^2$ values and 34 variables. The striking structural motifs in the $Ce_2Ru_4Mg_{17}$ structure are slightly bent $CeRu_2$ units with short Ce–Ru distances of 231 pm and additionally a short Ce–Ce distance of 307 pm. These features are a direct consequence of the cerium valence. The $CeRu_2$ units are embedded in a magnesium-rich matrix with a broad range of Mg–Mg distances (291 – 361 pm). Temperature-dependent magnetic susceptibility data show intermediate-valent behavior of the cerium atoms (0.23(5) $\mu_B$ per Ce atom) and no magnetic ordering down to 3 K, indicative of almost tetravalent cerium in $Ce_2Ru_4Mg_{17}$. The cerium-rich gallide $Ce_9Ru_4Ga_5$ shows an unusually short Ce–Ru distance of 237 pm for the Ce2 position as a result of an intermediate cerium valence. The structural distortions are discussed on the basis of a group-subgroup scheme for $La_9Ru_4In_5$ (space group $I4/mmm$) and the superstructure variant $Ce_9Ru_4Ga_5$ (space group $I4mm$).

*Key words:* Intermetallics, Cerium, Intermediate Valence, Group-Subgroup Relation

## Introduction

Extremely short Ce–Ru distances associated with strong covalent Ce–Ru bonding have recently been observed in a variety of intermetallic $Ce_xRu_yX_z$ ($X$ = Al, Ga, In, Sn, Mg, Cd, Zn) compounds [1, 2]. The short Ce–Ru distances are directly coupled with intermediate cerium valence for the involed cerium atoms, leading to a $(4-\delta)+$ oxidation state with only marginally filled $4f$ states. The structures of the diverse $Ce_xRu_yX_z$ intermetallics differ drastically. $CeRu_{0.88}In_2$ [3] and $CeRu_2Mg_5$ [4] have only one crystallographic cerium site, both with short Ce–Ru distances of 253 ($CeRu_{0.88}In_2$) and 232 ($CeRu_2Mg_5$) pm, distinctly shorter than the sum of the covalent radii [5] of 289 pm. The structures of CeRuSn [6], $Ce_3Ru_2In_3$ [7], and $Ce_2RuZn_4$ [8] show an ordering of purely trivalent and intermediate-valent cerium on two distinct Wyckoff sites. More complex behavior occurs for $Ce_5Ru_3Al_2$ [9], $Ce_{11}Ru_2Al_6$ [10], and $Ce_{23}Ru_7Mg_4$ [11], which contain 4, 6, respectively 9 crystallographically different cerium sites with a broad range of Ce–Ru distances. The strong covalent $Ce^{\sim IV}$–Ru bonding was also manifested through electronic structure calculations for CeRuSn [12] and $Ce_2RuZn_4$ [13].

In continuation of our systematic phase analytical investigations of rare earth metal-transition metal-magnesium systems [14], besides $Ce_4RuMg$ [15], $Ce_{23}Ru_7Mg_4$ [11], and $CeRu_2Mg_5$ [4] we now obtained the fourth phase, $Ce_2Ru_4Mg_{17}$ in the Ce–Ru–Mg system. $Ce_2Ru_4Mg_{17}$ is a further example for an intermediate-valent cerium compound with extremely short Ce–Ru distances. The synthesis, structure determination and the magnetic properties of this peculiar compound are reported herein. Additionally we worked out a group-subgroup scheme for the structures of $La_9Ru_4In_5$ and $Ce_9Ru_4Ga_5$ [16] which relates the structural distortions to the formation of short Ce–Ru bonds.

## Experimental Section

### *Synthesis*

Starting materials for the preparation of $Ce_2Ru_4Mg_{17}$ were a cerium ingot (Johnson Matthey, > 99.9 %), ruthenium powder (Allgemeine Gold- und Silberscheideanstalt Pforzheim, > 99.99 %) and a magnesium rod (Alpha Aesar,

> 99.8 %; the surface layer of the rod was removed on a turning lathe). The larger cerium ingot was first cut into smaller pieces and arc-melted [17] to a small button under an argon atmosphere of *ca.* 700 mbar. The argon was purified with titanium sponge (900 K), silica gel, and molecular sieves. A cerium button, ruthenium powder, and small magnesium pieces were weighed in the ideal 2 : 4 : 17 atomic ratio and arc-welded in a tantalum tube under an argon pressure of 700 mbar. The tantalum tube was then placed in the water-cooled sample chamber of an induction furnace [18] (Hüttinger Elektronik, Freiburg, Germany, Typ TIG 2.5/300), rapidly heated to 1370 K, kept at that temperature for 10 min and quenched by switching off the power supply. The temperature was controlled by a Sensor Therm Methis MS09 pyrometer with an accuracy of ±30 K. The polycrystalline $Ce_2Ru_4Mg_{17}$ sample is brittle. It could easily be separated from the tantalum container, and we observed no reaction with the crucible material. $Ce_2Ru_4Mg_{17}$ is stable in air.

*EDX data*

The $Ce_2Ru_4Mg_{17}$ crystal studied on the diffractometer was investigated by semiquantitative EDX analyses by use of a Zeiss EVO MA10 scanning electron microscope (variable pressure mode) with $CeO_2$, Ru, and MgO as standards. The experimentally observed composition (11 ± 3 at.-% Ce : 19 ± 3 at.-% Ru : 70 ± 3 at.-% Mg) was close to the ideal one (8.7 : 17.4 : 73.9). No impurity elements were found.

*X-Ray diffraction*

The polycrystalline $Ce_2Ru_4Mg_{17}$ sample was characterized by powder X-ray diffraction: Guinier camera (imaging plate detector, Fujifilm BAS-1800 readout system), Cu$K_{\alpha 1}$ radiation and $\alpha$-quartz ($a$ = 491.30 and $c$ = 540.46 pm) as the internal standard. The tetragonal lattice parameters (Table 1) were obtained from a least-squares refinement of the powder diffraction data. An intensity calculation [19] with the atomic positions from the structure refinement helped to ensure correct indexing.

Irregularly shaped single crystals of $Ce_2Ru_4Mg_{17}$ were obtained from the crushed sample prepared in the induction furnace. The crystal quality was first checked by Laue photographs on a Buerger camera (white Mo radiation) in order to test the quality for intensity data collection. Intensity data were collected at r. t. and additionally at 90 K (for a different crystal) by use of a Stoe IPDS-II imaging plate diffractometer in oscillation mode (graphite-monochromatized Mo$K_\alpha$ radiation). A numerical absorption correction was applied to the data sets. All relevant details concerning the data collections and evaluations are listed in Table 1.

*Structure refinement*

The r. t. data set was evaluated first. The data set showed a body-centered tetragonal lattice with high Laue symmetry and no further systematic extinctions, leading to the possible space groups $I4/mmm$, $I4mm$, $I\bar{4}2m$, and $I\bar{4}m2$, of which the non-centrosymmetric group $I\bar{4}2m$ was found to be correct during structure refinement. The starting atomic parameters were then determined *via* Direct Methods with SHELXS-97 [20], and the structure was refined using SHELXL-97 [21] (full-matrix least-squares on $F^2$) with anisotropic atomic displacement parameters for all sites. As a check for the correct composition, the occupancy parameters were refined in a separate series of least-squares cycles. All sites were fully occupied within two standard deviations, and in the final cycles the ideal values were assumed again. Refinement of the correct absolute structure was ensured through calculation of the Flack parameter [22, 23]. Refinement of the 90 K data set led to similar results, except for the opposite absolute structure, since a different crystal was measured. The final difference Fourier syntheses were flat (Table 1). The positional parameters and interatomic distances (exemplarily for the room temperature data) are listed in Tables 2 and 3.

Table 1. Crystal data and structure refinement for $Ce_2Ru_4Mg_{17}$, space group $I\bar{4}2m$, $Z$ = 2, $M$ = 1097.79 g mol$^{-1}$.

| Temperature, K | 293 | 90 |
|---|---|---|
| Unit cell dimensions | | |
| $a$, pm | 986.75(8) | 985.51(8) |
| $c$, pm | 1008.7(1) | 1004.3(1) |
| Cell volume $V$, nm$^3$ | 0.9822 | 0.9754 |
| Calculated density, g cm$^{-3}$ | 3.71 | 3.74 |
| Crystal size, $\mu$m$^3$ | 20 × 60 × 60 | 10 × 20 × 60 |
| Transm. ratio (max / min) | 0.852 / 0.619 | 0.901 / 0.807 |
| Absorption coefficient, mm$^{-1}$ | 8.1 | 8.1 |
| Detector distance, mm | 80 | 80 |
| Exposure time, min | 8 | 20 |
| $\omega$ range; increment, deg | 0 – 180, 1.0 | 0 – 180, 1.0 |
| Integr. param. A, B, EMS | 12.2; 2.4; 0.012 | 13.0; 3.0; 0.013 |
| $F$(000), e | 992 | 992 |
| $\theta$ range for data collection, deg | 2 – 32 | 2 – 32 |
| Range in $hkl$ | ±14, ±14, ±14 | ±14, ±14, ±14 |
| Total no. reflections | 5039 | 5952 |
| Independent reflections / $R_{int}$ | 909 / 0.0685 | 901 / 0.0576 |
| Reflections with $I \geq 2\sigma(I)$ / $R_\sigma$ | 689 / 0.0834 | 804 / 0.0374 |
| Data / ref. parameters | 909 / 34 | 901 / 34 |
| $R1$ / $wR2$ for $I \geq 2\sigma(I)$ | 0.0343 / 0.0479 | 0.0278 / 0.0501 |
| $R1$ / $wR2$ for all data | 0.0601 / 0.0513 | 0.0354 / 0.0513 |
| Goodness-of-fit on $F^2$ | 0.856 | 1.043 |
| Extinction coefficient | 0.00046(8) | 0.00025(12) |
| Flack parameter | −0.03(4) | −0.04(3) |
| Largest diff. peak / hole, e Å$^{-3}$ | 3.57 / −3.38 | 2.22 / −1.17 |

Further details of the crystal structure investigation may be obtained from Fachinformationszentrum Karlsruhe, 76344 Eggenstein-Leopoldshafen, Germany (fax: +49-7247-808-666; e-mail: crysdata@fiz-karlsruhe.de, http://www.fiz-karlsruhe.de/request_for_deposited_data.html) on quoting the deposition number CSD-424260 (293 K data) and CSD-424261 (90 K data).

Table 2. Atomic coordinates and anisotropic displacement parameters ($pm^2$) for $Ce_2Ru_4Mg_{17}$. $U_{eq}$ is defined as one third of the trace of the orthogonalized $U_{ij}$ tensor. The anisotropic displacement factor exponent takes the form: $-2\pi^2[(ha*)2U_{11} + \cdots + 2hka*b*U_{12}]$.

| Atom | Wyckoff position | $x$ | $y$ | $z$ | $U_{11}$ | $U_{22}$ | $U_{33}$ | $U_{23}$ | $U_{13}$ | $U_{12}$ | $U_{eq}$ |
|---|---|---|---|---|---|---|---|---|---|---|---|
| 293 K data | | | | | | | | | | | |
| Ce | 4*e* | 0 | 0 | 0.65238(14) | 143(3) | $U_{11}$ | 659(8) | 0 | 0 | 58(4) | 315(3) |
| Ru | 8*i* | 0.65512(5) | $x$ | 0.83278(9) | 91(2) | $U_{11}$ | 107(3) | 9(3) | $U_{23}$ | −5(3) | 96(1) |
| Mg1 | 2*a* | 0 | 0 | 0 | 229(29) | $U_{11}$ | 990(87) | 0 | 0 | 0 | 483(28) |
| Mg2 | 8*g* | 0.6798(4) | 0 | 1/2 | 201(17) | 150(16) | 157(15) | −11(16) | 0 | 0 | 169(7) |
| Mg3 | 8*i* | 0.7842(3) | $x$ | 0.0687(3) | 181(11) | $U_{11}$ | 154(16) | −61(10) | $U_{23}$ | 51(14) | 172(7) |
| Mg4 | 16*j* | 0.7025(2) | 0.9455(2) | 0.8099(2) | 193(12) | 125(11) | 151(14) | 16(9) | 7(9) | −29(9) | 156(6) |
| 90 K data | | | | | | | | | | | |
| Ce | 4*e* | 0 | 0 | 0.35007(7) | 59(2) | $U_{11}$ | 244(4) | 0 | 0 | 15(2) | 120(2) |
| Ru | 8*i* | 0.33406(4) | $x$ | 0.16572(6) | 46(1) | $U_{11}$ | 55(2) | 5(2) | $U_{23}$ | 0(2) | 49(1) |
| Mg1 | 2*a* | 0 | 0 | 0 | 59(13) | $U_{11}$ | 385(35) | 0 | 0 | 0 | 167(12) |
| Mg2 | 8*g* | 0.3218(2) | 0 | 1/2 | 77(9) | 50(9) | 89(10) | 8(10) | 0 | 0 | 72(4) |
| Mg3 | 8*i* | 0.2163(2) | $x$ | 0.9309(3) | 94(7) | $U_{11}$ | 74(11) | −28(7) | $U_{23}$ | 20(8) | 87(5) |
| Mg4 | 16*j* | 0.2963(2) | 0.0540(2) | 0.1899(2) | 95(8) | 62(7) | 70(9) | −6(6) | 1(6) | −12(6) | 76(4) |

*Physical property measurements*

A compact piece of $Ce_2Ru_4Mg_{17}$ weighing 7.219 mg was enclosed in kapton foil and attached to the sample holder rod of a VSM for measuring the magnetic properties in a Quantum Design Physical-Property-Measurement System in the temperature range of 3 – 300 K with a magnetic flux density of 10 kOe.

## Discussion

*Crystal chemistry of $Ce_2Ru_4Mg_{17}$*

Besides $CeRu_2Mg_5$ [4], $Ce_{23}Ru_7Mg_4$ [11] and $Ce_4RuMg$ [15], $Ce_2Ru_4Mg_{17}$ is already the fourth compound reported in the ternary system Ce-Ru-Mg. So far, only the Ce-Ru-In system [24, and refs. therein] shows more phases. $Ce_2Ru_4Mg_{17}$ crystallizes with its own, singular structure type, similar to many other $Ce_xRu_yX_z$ intermetalics with short Ce–Ru distances [1, 2]. The striking structural motif in the $Ce_2Ru_4Mg_{17}$ structure is the formation of slightly bent Ru–Ce–Ru units with Ce–Ru distances of 231 pm, significantly shorter than the sum of the covalent radii [5] of 289 pm. The near-neighbor coordination of one Ru–Ce–Ru unit is presented in Fig. 1. There are very large similarities with the corresponding unit in $CeRu_2Mg_5$ [4]. In the latter compound the Ru–Ce–Ru unit is slightly more bent, and we observe two cerium neighbors instead of one cerium and one magnesium atom in $Ce_2Ru_4Mg_{17}$. The cerium and ruthenium atoms in $Ce_2Ru_4Mg_{17}$ form slightly distorted tetrahedral units. The packing of these $Ce_2Ru_4$ units in $Ce_2Ru_4Mg_{17}$ is presented in Fig. 2. The cerium pairs are aligned on the $\bar{4}$ axis.

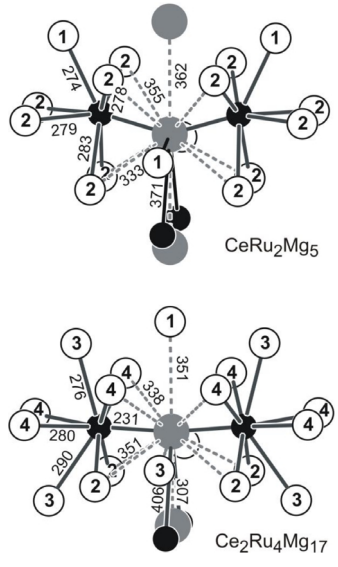


Fig. 1. Cut-outs of the $CeRu_2Mg_5$ (top) and $Ce_2Ru_4Mg_{17}$ (bottom) structures. Cerium, ruthenium, and magnesium atoms are drawn as medium grey, black filled, and open circles, respectively. Relevant interatomic distances are indicated.

$Ce_2Ru_4Mg_{17}$ is the magnesium-richest compound in the Ce–Ru–Mg system. The four crystallographically independent magnesium sites have between 9 and 12 magnesium atoms in their coordination spheres (Table 3). The Mg1 atoms at the origin of the unit cell have the highest magnesium coordination number in the form of a strongly distorted cuboctahedron. The Mg–Mg distances cover the broad range from 291 to 361 pm. Similar to the structure of $CeRu_2Mg_5$ (302 – 341 pm Mg–Mg) [4], also in

Table 3. Interatomic distances (pm) in the structure of $Ce_2Ru_4Mg_{17}$. Standard deviations are given in parentheses.

| | | | 293 K | 90 K |
|---|---|---|---|---|
| Ce: | 2 | Ru | 230.9(1) | 231.8(1) |
| | 1 | Ce | 307.4(3) | 301.2(2) |
| | 4 | Mg4 | 338.1(2) | 337.6(2) |
| | 1 | Mg1 | 350.6(1) | 351.6(1) |
| | 4 | Mg2 | 351.4(3) | 351.1(2) |
| Ru: | 1 | Ce | 230.9(1) | 231.8(1) |
| | 1 | Mg3 | 275.6(3) | 275.4(3) |
| | 2 | Mg2 | 280.0(2) | 279.4(1) |
| | 2 | Mg4 | 280.1(2) | 279.5(2) |
| | 1 | Mg3 | 290.3(3) | 287.3(3) |
| | 2 | Mg4 | 291.1(2) | 290.7(2) |
| Mg1: | 4 | Mg3 | 309.0(4) | 309.3(3) |
| | 2 | Ce | 350.6(1) | 351.6(1) |
| | 8 | Mg4 | 354.7(2) | 352.8(2) |
| Mg2: | 2 | Ru | 280.0(2) | 279.4(1) |
| | 2 | Mg3 | 291.1(2) | 290.6(2) |
| | 2 | Mg4 | 303.3(2) | 302.8(2) |
| | 2 | Mg4 | 318.0(2) | 317.0(2) |
| | 2 | Ce | 351.4(3) | 351.1(2) |
| | 1 | Mg2 | 354.8(7) | 351.2(5) |
| | 2 | Mg4 | 360.8(3) | 359.2(3) |
| Mg3: | 1 | Ru | 275.6(3) | 275.4(3) |
| | 1 | Ru | 290.3(3) | 287.3(3) |
| | 2 | Mg2 | 291.1(2) | 290.6(2) |
| | 2 | Mg4 | 304.3(3) | 303.1(2) |
| | 1 | Mg1 | 309.0(4) | 309.3(3) |
| | 2 | Mg4 | 316.2(4) | 315.3(3) |
| | 2 | Mg4 | 332.8(4) | 331.7(3) |
| Mg4: | 1 | Ru | 280.1(2) | 279.6(2) |
| | 1 | Ru | 291.1(2) | 290.7(2) |
| | 1 | Mg2 | 303.3(2) | 302.8(2) |
| | 1 | Mg3 | 304.3(3) | 303.1(2) |
| | 1 | Mg3 | 316.2(4) | 315.3(3) |
| | 2 | Mg4 | 316.7(3) | 317.6(3) |
| | 1 | Mg2 | 318.0(2) | 317.0(2) |
| | 1 | Mg3 | 332.8(4) | 331.7(3) |
| | 1 | Ce | 338.1(2) | 337.6(2) |
| | 1 | Mg4 | 339.0(5) | 337.6(4) |
| | 1 | Mg1 | 354.7(2) | 352.8(2) |
| | 1 | Mg2 | 360.8(3) | 359.2(2) |

$Ce_2Ru_4Mg_{17}$ we observe Mg–Mg distances which are slightly shorter than in *hcp* magnesium (320 pm average Mg–Mg) [25]. This is the typical range for magnesium-rich $RE_xT_yMg_z$ intermetallics [26, 27]. Besides the already mentioned short Ce–Ru contact, each ruthenium atom has eight magnesium neighbors at Ru–Mg distances ranging from 276 to 291 pm, longer than the sum of the covalent radii [5] of 260 pm. Again, this range is close to that found in the structures of $CeRu_2Mg_5$ (273 – 283 pm Ru–Mg) [4] and binary $Ru_2Mg_3$ (282 – 296 pm) [28].

A second striking structural feauture of the $Ce_2Ru_4Mg_{17}$ structure, besides the short Ce–Ru distances, are the extremely short Ce–Ce distances

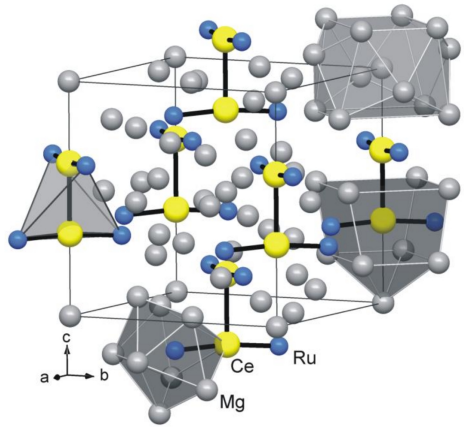


Fig. 2 (color online). The unit cell of $Ce_2Ru_4Mg_{17}$. Some striking structural units are emphasized. For details see text.

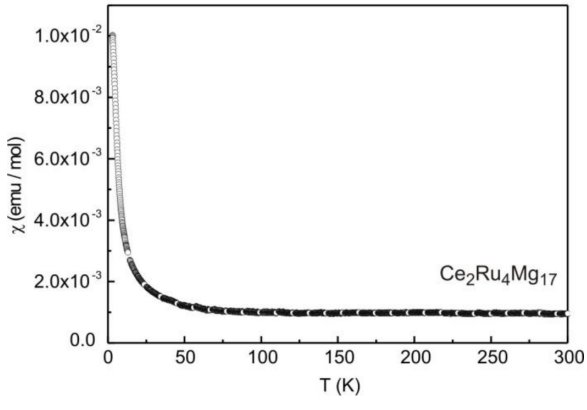


Fig. 3. Temperature dependence of the magnetic susceptibility ($\chi$ data) of $Ce_2Ru_4Mg_{17}$ measured at 10 kOe.

of 307 pm, much shorter than in *fcc* cerium (365 pm) [25] and well beyond the Hill limit of 340 pm for $f$ electron localization [29]. This is a consequence of the non-magnetic ground state (almost tetravalent cerium) that is evident from the temperature-dependent susceptibility measurements (*vide infra*), indicating a small effective size of cerium. Such short Ce–Ce distances, accompanied by intermediate-valent cerium have also been observed for other cerium intermetallics, *e. g.* $CeRu_3B_2$ (299.1 pm) [30], $CeCo_3B_2$ (303.6 pm) [31], $CeCo_2$ (309.4 pm) [32, 33], $CeCo_3$ (314 pm) [34], or $Ce_4Ru_3$ (312 pm) [35].

As is evident from Table 2, the occurrence of almost tetravalent cerium in $Ce_2Ru_4Mg_{17}$ is directly accompanied by strong anisotropic displacements of the cerium and also of the adjacent Mg1 atoms which are all aligned parallel to the $c$ axis.

| La1:16*n* | La2:2*a* | Ru1:8*i* | In1:8*h* | In2:2*b* |
|---|---|---|---|---|
| .*m*. | 4/*mmm* | *m*2*m*. | *m*.2*m* | 4/*mmm* |
| 0 | 0 | 0.3703 | 0.2186 | 0 |
| 0.2727 | 0 | 0 | *x* | 0 |
| 0.2979 | 0 | 0 | 0 | 1/2 |

*I*4/*mmm* $RE_9Ru_4X_5$

t2
-0.1929

*I*4*mm* $Ce_9Ru_4Ga_5$

*averaged*

| Ce2:16*n* | Ce1:2*a* | Ru:8*i* | Ga2:8*h* | Ga1:2*b* |
|---|---|---|---|---|
| .*m*. | 4/*mmm* | *m*2*m*. | *m*.2*m* | 4/*mmm* |
| 0.2669 | 0 | 0.3516 | 0.2202 | 0 |
| 0 | 0 | 0 | *x* | 0 |
| 0.3071 | 0 | 0 | 0 | 1/2 |

*calculated*

| Ce2:8*d* | Ce3:8*d* | Ce1:2*a* | Ru:8*d* | Ga2:8*c* | Ga1:2*a* |
|---|---|---|---|---|---|
| .*m*. | .*m*. | 4*mm* | .*m*. | ..*m* | 4*mm* |
| 0.2669 | 0.2669 | 0 | 0.3516 | 0.2202 | 0 |
| 0 | 0 | 0 | 0 | *x* | 0 |
| 0.5000 | 0.8858 | 0.1929 | 0.1929 | 0.1929 | 0.6929 |

*refined*

| Ce2:8*d* | Ce3:8*d* | Ce1:2*a* | Ru:8*d* | Ga2:8*c* | Ga1:2*a* |
|---|---|---|---|---|---|
| .*m*. | .*m*. | 4*mm* | .*m*. | ..*m* | 4*mm* |
| 0.2791 | 0.2547 | 0 | 0.3516 | 0.2202 | 0 |
| 0 | 0 | 0 | 0 | *x* | 0 |
| 0.5000 | 0.8859 | 0.2216 | 0.2230 | 0.1908 | 0.6536 |

Fig. 4. Group-subgroup scheme in the Bärnighausen formalism [36 – 39] for the structures of $La_9Ru_4In_5$ and $Ce_9Ru_4Ga_5$ [16]. The index for the *translationengleiche* (t) symmetry reduction, the unit cell transformation, and the evolution of the atomic parameters are given. The averaged positional parameters were calculated from the refined values.

At 90 K the anisotropic displacement parameters $U_{33}$ of Ce and Mg1 were still by a factor of $\sim 6$ higher as compared to the $U_{33}$ values of the other atoms. The slope of the decrease, however, is comparable suggesting no change of symmetry down to 90 K.

*Magnetic properties of $Ce_2Ru_4Mg_{17}$*

Fig. 3 displays the temperature dependence of the magnetic susceptibility ($\chi$ data) of $Ce_2Ru_4Mg_{17}$ measured at a field strength of 10 kOe. The magnetic susceptibility is nearly temperature-independent in the range of 75 – 300 K, which classifies the compound as a Pauli paramagnet. At temperatures below 75 K the TIP is superimposed by a paramagnetic component, which could either be caused by a minor impurity or be due to the fact that the $f$ shell of the cerium atoms is still partially occupied, *i. e.* a small localized magnetic moment is present. Fitting of the data using the modified Curie-Weiss law results in an effective magnetic moment of $\mu_{\text{eff}} = 0.23(5)\ \mu_B$ per Ce atom, a Weiss constant of $\theta_p = -10.5(5)$ K and a temperature-independent term of $\chi_0 = 8.9(1) \times 10^{-4}$ emu mol$^{-1}$. The small magnetic moment shows that the cerium atoms are in a nearly tetravalent oxidation state, which is also in line with the observed short Ce–Ru and Ce–Ce distances.

*A group-subgroup scheme for $La_9Ru_4In_5$ and $Ce_9Ru_4Ga_5$*

The intermediate cerium valence in $Ce_xRu_yX_z$ intermetallics drastically influences the Ce–Ru coordination. Thus, in most cases it is not possible to enable such a peculiar environment with the neighboring rare earth elements lanthanum and praseodymium. Consequently one observes two ways out, *i. e.* (i) the cerium compound crystallizes with its unique structure type as a singular compound or (ii) formation of a superstructure through lowering of the space group symmetry, allowing for an ordering of trivalent and intermediate-valent cerium. Two examples for such superstructures are CeRuSn [6], which adopts a superstructure of CeCoAl upon doubling of the subcell

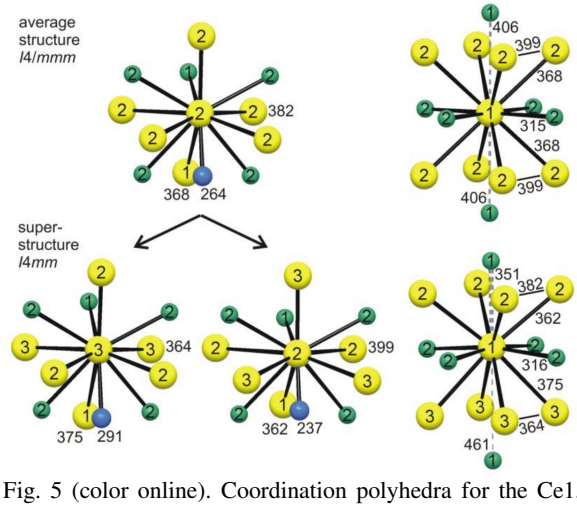


Fig. 5 (color online). Coordination polyhedra for the Ce1, Ce2, and Ce3 atoms in $Ce_9Ru_4Ga_5$ (bottom), space group *I*4*mm* and the calculated average subcell structure (top), space group *I*4/*mmm*. Atom designations and relevant interatomic distances are indicated.

*c* axis, and rhombohedral $Ce_5Ru_3Al_2$ [2, 9], a superstructure of cubic $Pr_5Ru_3Al_2$ [9].

The recently reported indide $La_9Ru_4In_5$ (space group $I4/mmm$) and the gallide $Ce_9Ru_4Ga_5$ (space group $I4mm$) [16] are another pair of new structure types which are directly related by a group-subgroup scheme. The latter is presented in the concise and compact Bärnighausen formalism [36 – 39] in Fig. 4. Due to simple decentering (*translationengleiche* symmetry reduction of index 2 from $I4/mmm$ to $I4mm$), the 16*n* La site splits into two eightfold sites 8*d* for cerium, enabling the trivalent-intermediate-valent cerium ordering accompanied by significant distortions in the $Ce^{\sim IV}$ coordination. The corresponding coordination polyhedra and relevant interatomic distances are shown in Fig. 5. The intermediate cerium valence in $Ce_9Ru_4Ga_5$ had been confirmed experimentally by $L_3$-Ce XANES spectra [9].

*Acknowledgement*

This work was financially supported by the Deutsche Forschungsgemeinschaft.

[1] W. Hermes, S. F. Matar, R. Pöttgen, *Z. Naturforsch.* **2009**, *64b*, 901.
[2] T. Mishra, R.-D. Hoffmann, C. Schwickert, R. Pöttgen, *Z. Naturforsch.* **2011**, *66b*, 771.
[3] E. V. Murashova, A. I. Tursina, Zh. M. Kurenbaeva, A. V. Gribanov, Yu. D. Seropegin, *J. Alloys Compd.* **2008**, *454*, 206.
[4] S. Linsinger, M. Eul, U. Ch. Rodewald, R. Pöttgen, *Z. Naturforsch.* **2010**, *65b*, 1185.
[5] J. Emsley, *The Elements*, Oxford University Press, Oxford **1999**.
[6] J. F. Riecken, W. Hermes, B. Chevalier, R. -D. Hoffmann, F. M. Schappacher, R. Pöttgen, *Z. Anorg. Allg. Chem.* **2007**, *633*, 1094.
[7] Zh. M. Kurenbaeva, A. I. Tursina, E. V. Murashova, S. N. Nesterenko, A. V. Gribanov, Yu. D. Seropegin, H. Noël, *J. Alloys Compd.* **2007**, *442*, 86.
[8] R. Mishra, W. Hermes, U. Ch. Rodewald, R.-D. Hoffmann, R. Pöttgen, *Z. Anorg. Allg. Chem.* **2008**, *634*, 470.
[9] E. V. Murashova, A. I. Tursina, N. G. Bukhanko, S. N. Nesterenko, Zh. M. Kurenbaeva, Y. D. Seropegin, H. Noël, M. Potel, T. Roisnel, D. Kaczorowski, *Mater. Res. Bull.* **2010**, *45*, 993.
[10] E. V. Murashova, A. I. Tursina, Zh. M. Kurenbaeva, H. Noël, Y. D. Seropegin, *Chem. Met. Alloys* **2010**, *3*, 101.
[11] S. Linsinger, M. Eul, W. Hermes, R.-D. Hoffmann, R. Pöttgen, *Z. Naturforsch.* **2009**, *64b*, 1345.
[12] S. F. Matar, J. F. Riecken, B. Chevalier, R. Pöttgen, A. F. Al. Alam, V. Eyert, *Phys. Rev. B* **2007**, *76*, 174434.
[13] V. Eyert, E.-W. Scheidt, W. Scherer, W. Hermes, R. Pöttgen, *Phys. Rev. B* **2008**, *78*, 214420.
[14] U. Ch. Rodewald, B. Chevalier, R. Pöttgen, *J. Solid State Chem.* **2007**, *180*, 1720.
[15] F. Tappe, C. Schwickert, S. Linsinger, R. Pöttgen, *Monatsh. Chem.* **2011**, *142*, 1087.
[16] K. Shablinskaya, E. Murashova, A. Tursina, Z. Kurenbaeva, A. Yaroslavtsev, Y. Seropegin, *Intermetallics* **2012**, *23*, 106.
[17] R. Pöttgen, Th. Gulden, A. Simon, *GIT Labor-Fachzeitschrift* **1999**, *43*, 133.
[18] R. Pöttgen, A. Lang, R.-D. Hoffmann, B. Künnen, G. Kotzyba, R. Müllmann, B. D. Mosel, C. Rosenhahn, *Z. Kristallogr.* **1999**, *214*, 143.
[19] K. Yvon, W. Jeitschko, E. Parthé, *J. Appl. Crystallogr.* **1977**, *10*, 73.
[20] G. M. Sheldrick, SHELXS-97, Program for the Solution of Crystal Structures, University of Göttingen, Göttingen (Germany) **1997**. See also: G. M. Sheldrick, *Acta Crystallogr.* **1990**, *A46*, 467.
[21] G. M. Sheldrick, SHELXL-97, Program for the Refinement of Crystal Structures, University of Göttingen, Göttingen (Germany) **1997**. See also: G. M. Sheldrick, *Acta Crystallogr.* **2008**, *A64*, 112.
[22] H. D. Flack, G. Bernadinelli, *Acta Crystallogr.* **1999**, *A55*, 908.
[23] H. D. Flack, G. Bernadinelli, *J. Appl. Crystallogr.* **2000**, *33*, 1143.
[24] Zh. M. Kurenbaeva, A. I. Tursina, E. V. Murashova, S. N. Nesterenko, Y. D. Seropegin, *Russ. J. Inorg. Chem.* **2011**, *56*, 218.
[25] J. Donohue, *The Structures of the Elements,* Wiley, New York **1974**.
[26] P. Solokha, S. De Negri, V. Pavlyuk, A. Saccone, B. Marciniak, *J. Solid State Chem.* **2007**, *180*, 3066.
[27] P. Solokha, S. De Negri, V. Pavlyuk, A. Saccone, *Solid State Sci.* **2009**, *11*, 801.
[28] R. Pöttgen, V. Hlukhyy, A. Baranov, Yu. Grin, *Inorg. Chem.* **2008**, *47*, 6051.
[29] H. H. Hill in *Plutonium and other Actinides* (Ed.: W. N. Mines), *Nuclear Materials Series, AIME*, **1970**, *17*, 2.
[30] H. C. Ku, G. P. Meisner, F. Acker, D. C. Johnston, *Solid State Commun.* **1980**, *35*, 91.
[31] Y. B. Kuz'ma, P. I. Krypyakevych, N. S. Bilonizhko, *Dopov. Akad. Nauk Ukr. RSR, Ser. A* **1969**, 939.

[32] W. Fülling, K. Moeller, R. Vogel, *Z. Metallkd.* **1942**, *34*, 253.
[33] T. M. Seixas, J. M. Machado da Silva, *Physica B* **1999**, *269*, 362.
[34] W. Ostertag, *Trans. Met. Soc. AIME* **1967**, *239*, 690.
[35] M. L. Fornasini, A. Palenzona, *Z. Kristallogr.* **1992**, *200*, 57.
[36] H. Bärnighausen, *Commun. Math. Chem.* **1980**, *9*, 139.
[37] U. Müller, *Z. Anorg. Allg. Chem.* **2004**, *630*, 1519.
[38] U. Müller in *International Tables for Crystallography*, Vol. A1, *Symmetry relations between space groups*, (Eds.: H. Wondratschek, U. Müller), 2nd Ed., John Wiley, Chichester, **2010**, pp. 44 – 56.
[39] U. Müller, *Symmetriebeziehungen zwischen verwandten Kristallstrukturen*, Vieweg + Teubner, Wiesbaden, **2012**.